Bicc1 polymerization regulates the localization and silencing of bound mRNA

Benjamin Rothé[1], Lucia Leal-Esteban[1], Florian Bernet[1], Séverine Urfer[1], Nicholas Doerr[2], Thomas Weimbs[2], Justyna Iwaszkiewicz[3], and Daniel B. Constam[1]

[1]*Ecole Polytechnique Fédérale de Lausanne (EPFL) SV ISREC, Station 19, CH-1015 Lausanne, Switzerland*

[2]*Department of Molecular, Cellular, and Developmental Biology and Neuroscience Research Institute, University of California Santa Barbara, Santa Barbara, California 93106-9610*

[3]*Swiss Institute of Bioinformatics, University of Lausanne, Lausanne, Switzerland*

SUPPLEMENTAL MATERIAL

Figures S1 to S8

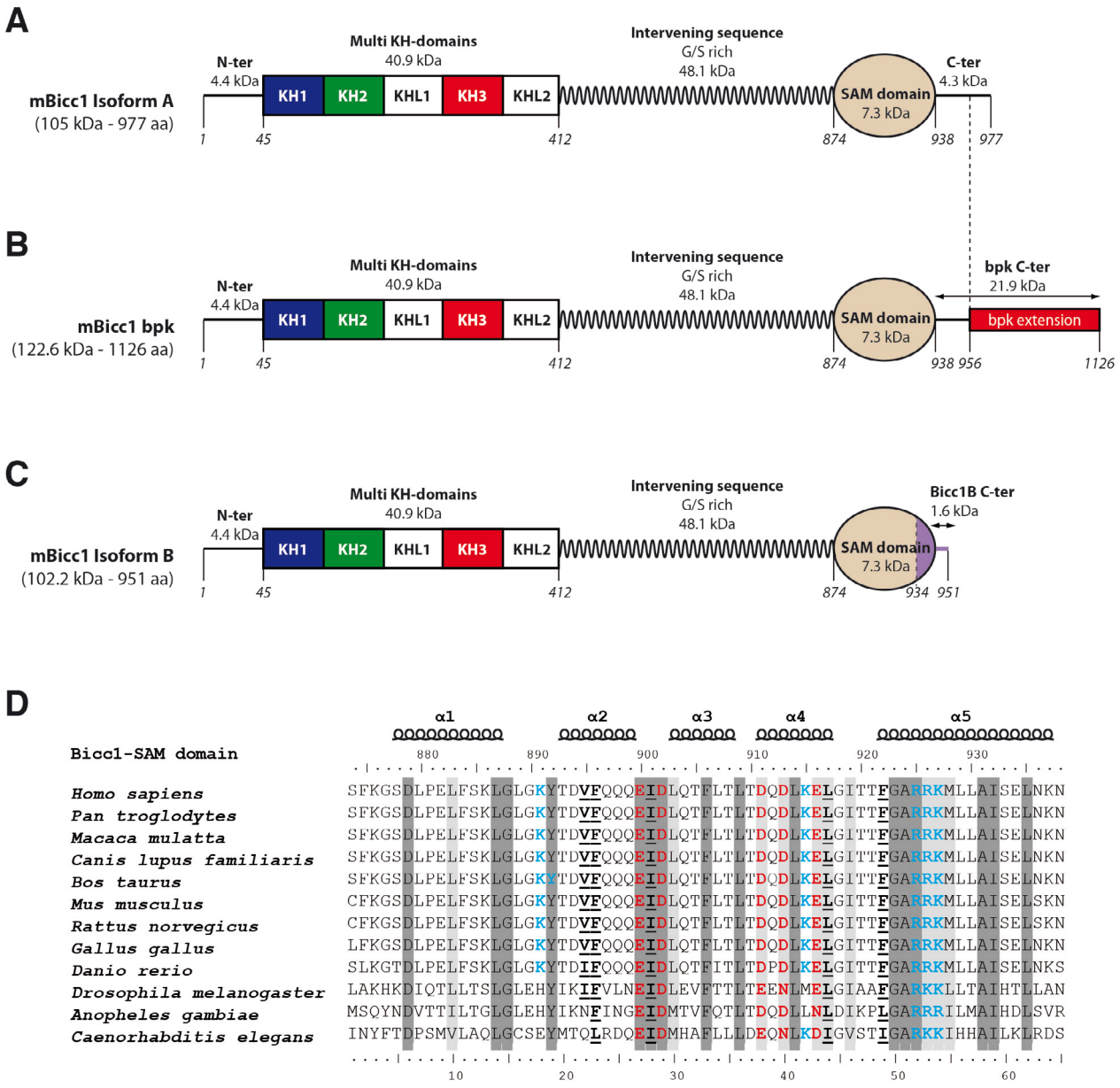

FIGURE S1: Detailed map of Bicc1 domains. (A, B, C) Schematic representation of Bicc1 isoform A, bpk and isoform B respectively and their molecular sizes. Bicc1 isoform B is characterized by the presence of a short penultimate exon 21 (134 nt) that includes a stop codon and thus shortens the C-terminu and changes the last five amino acids of the SAM domain (ELSKN) to VCDSV. The sequence of isoform B is unaffected by the *bpk* mutation that resides in exon 22. (D) Clustal-W alignment of the Bicc1 SAM domain and conserved sequences obtained with BioEdit software. According to the mouse Bicc1 SAM dimer model, residues of the ML (red) and EH surfaces (blue) and hydrophobic amino acids (underlined) are highlighted. The mouse Bicc1 sequence numbering is shown above the alignment.

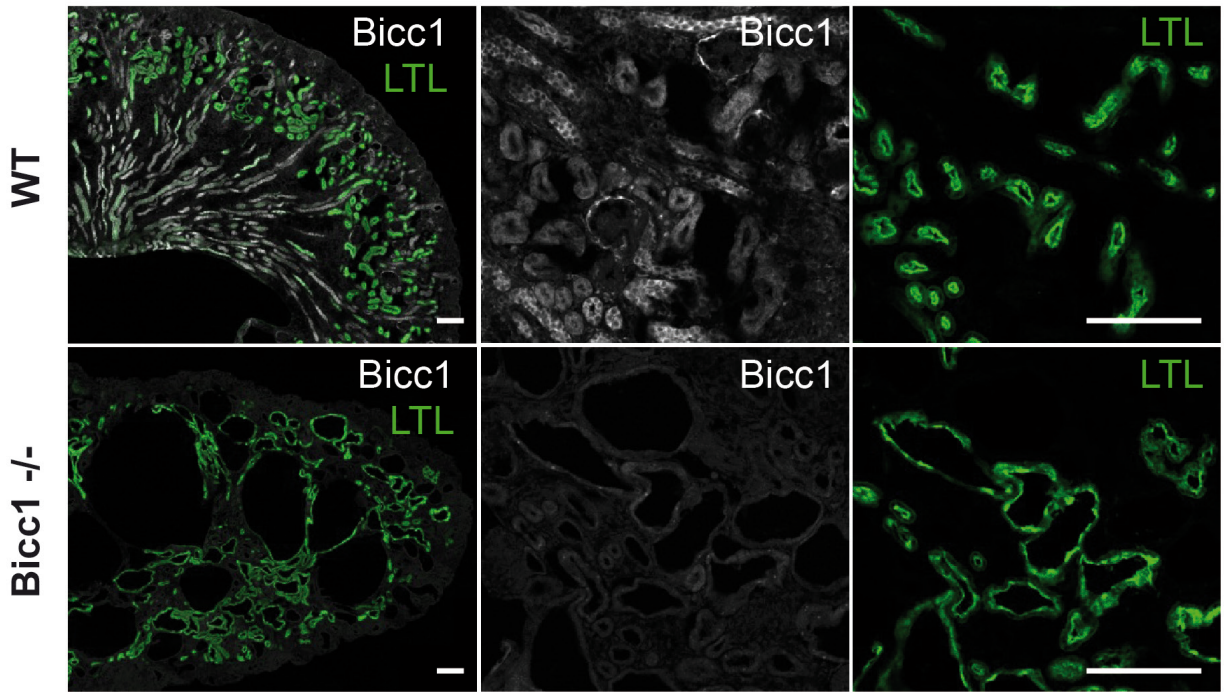

FIGURE S2: Characterization of a polyclonal anti-Bicc1 SAM domain antibody. Frozen sections of newborn wild-type (WT) and Bicc1-/- kidneys labeled with anti-SAM antibody. Cortical regions are shown at higher magnification on the right. Co-labeling with Lotus Tetragonolobus lectin (LTL) marks proximal tubules.

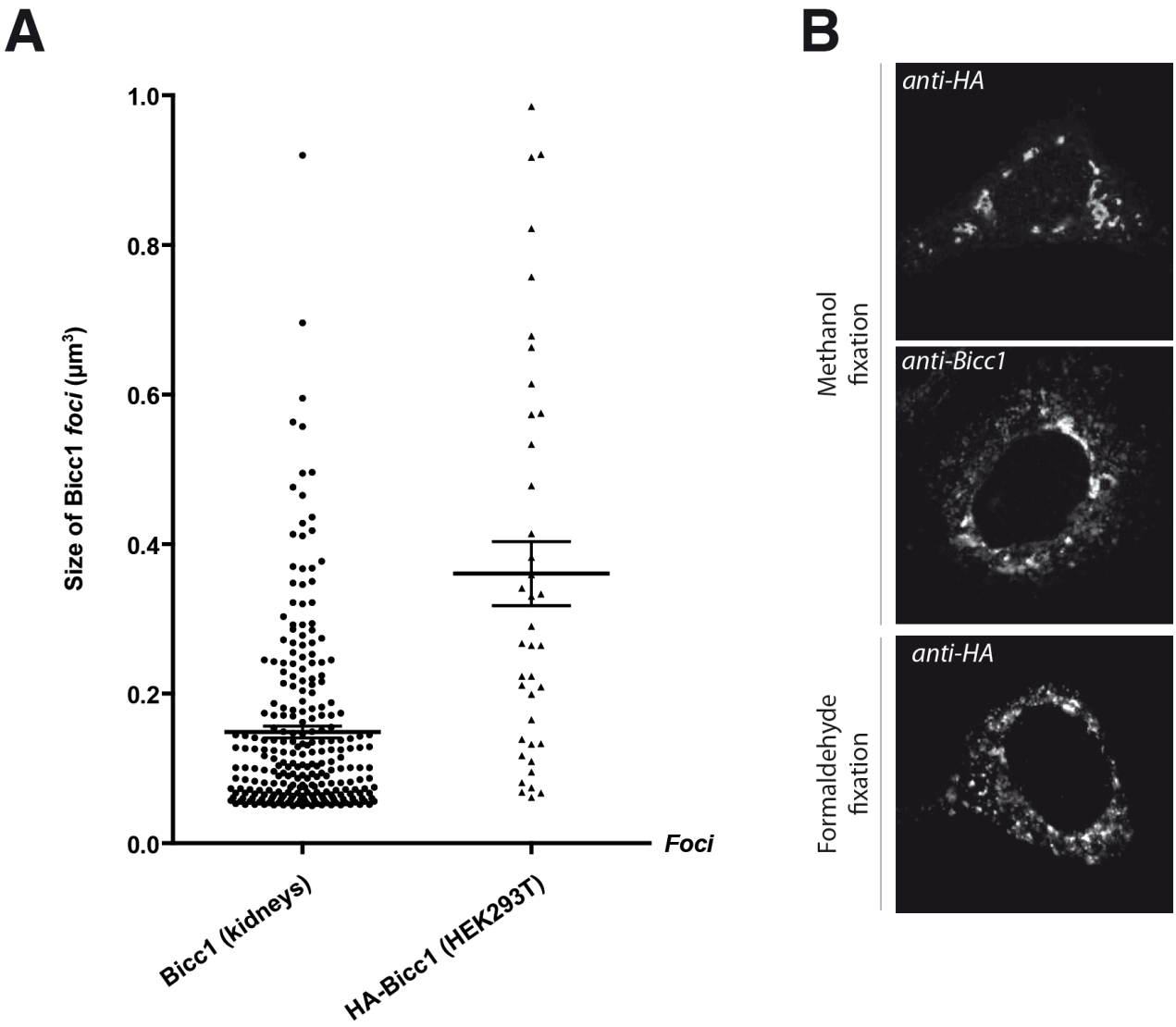

FIGURE S3: Size distribution of Bicc1 foci. (A) Graph comparing the volume (μm^3) distribution of Bicc1 foci and P-bodies in mouse tissues and HEK293T cells. Volume measurement were carried out from z-stack images using Imaris software. (B) Detection of Bicc1 foci in COS-1 cells by alternative immunostaining protocols. Methanol fixation and anti-HA antibody (upper panel) detected similar foci as those observed using a specific anti-Bicc1 antibody (middle panel) or using formaldehyde for fixation (bottom panel).

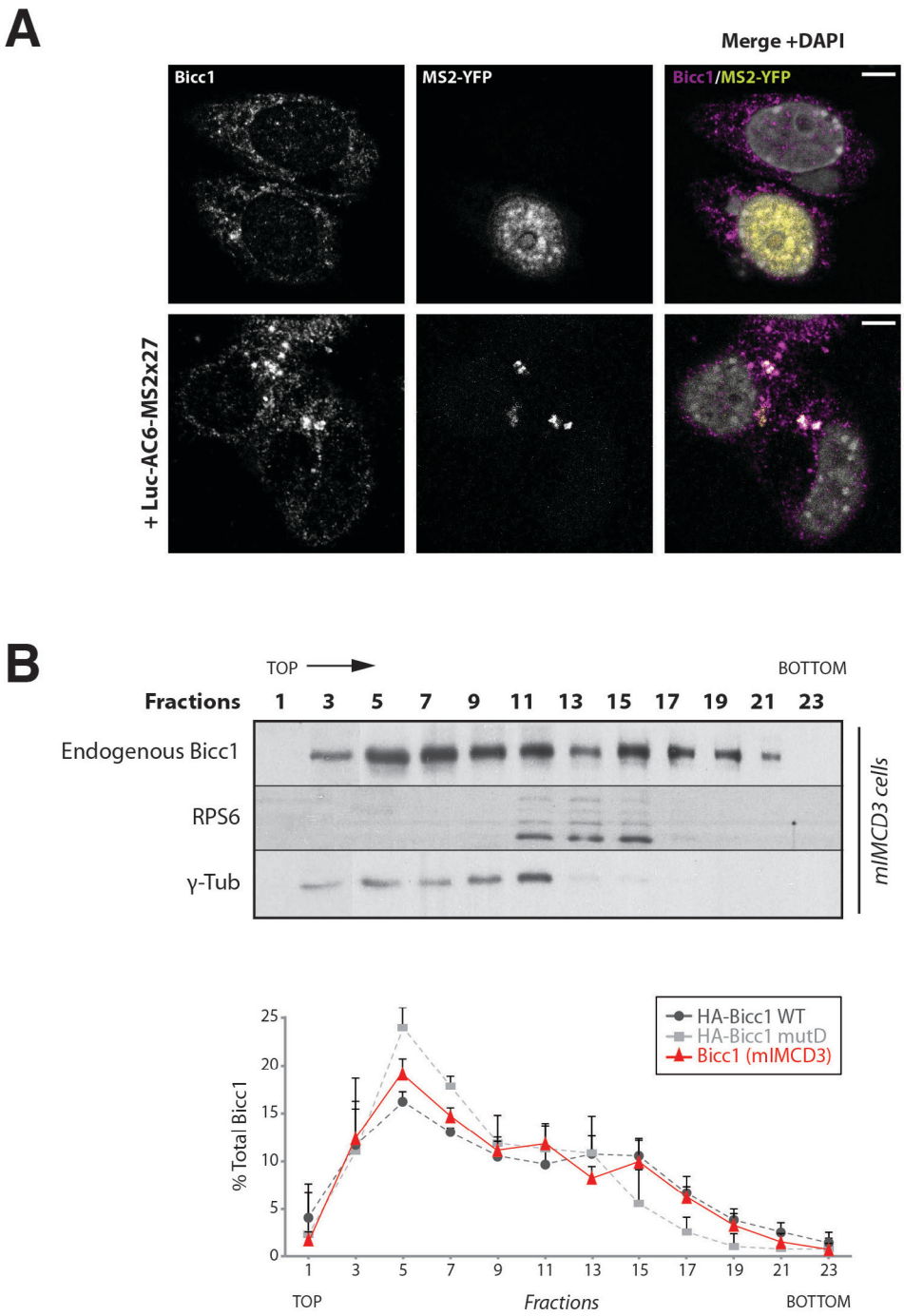

FIGURE S4: Endogenous Bicc1 from mIMCD3 cells assembles in large complexes and concentrates associated mRNA. (A) Localization by indirect immunofluorescence staining of the Luc-AC6-MS2x27 reporter mRNA and endogenous Bicc1 in mIMCD3 cells. Scale bar: 5 µM. (B) Density fractionation of endogenous Bicc1 on continuous 15-60% sucrose gradient. RPS6 and γ-tubulin were used as internal control. The graph below the gels shows the distribution of Bicc1 by comparison with HA-Bicc1 WT and mutant D (Figure 5A). Results represent mean values of three independent experiments. Error bars show standard error of the mean.

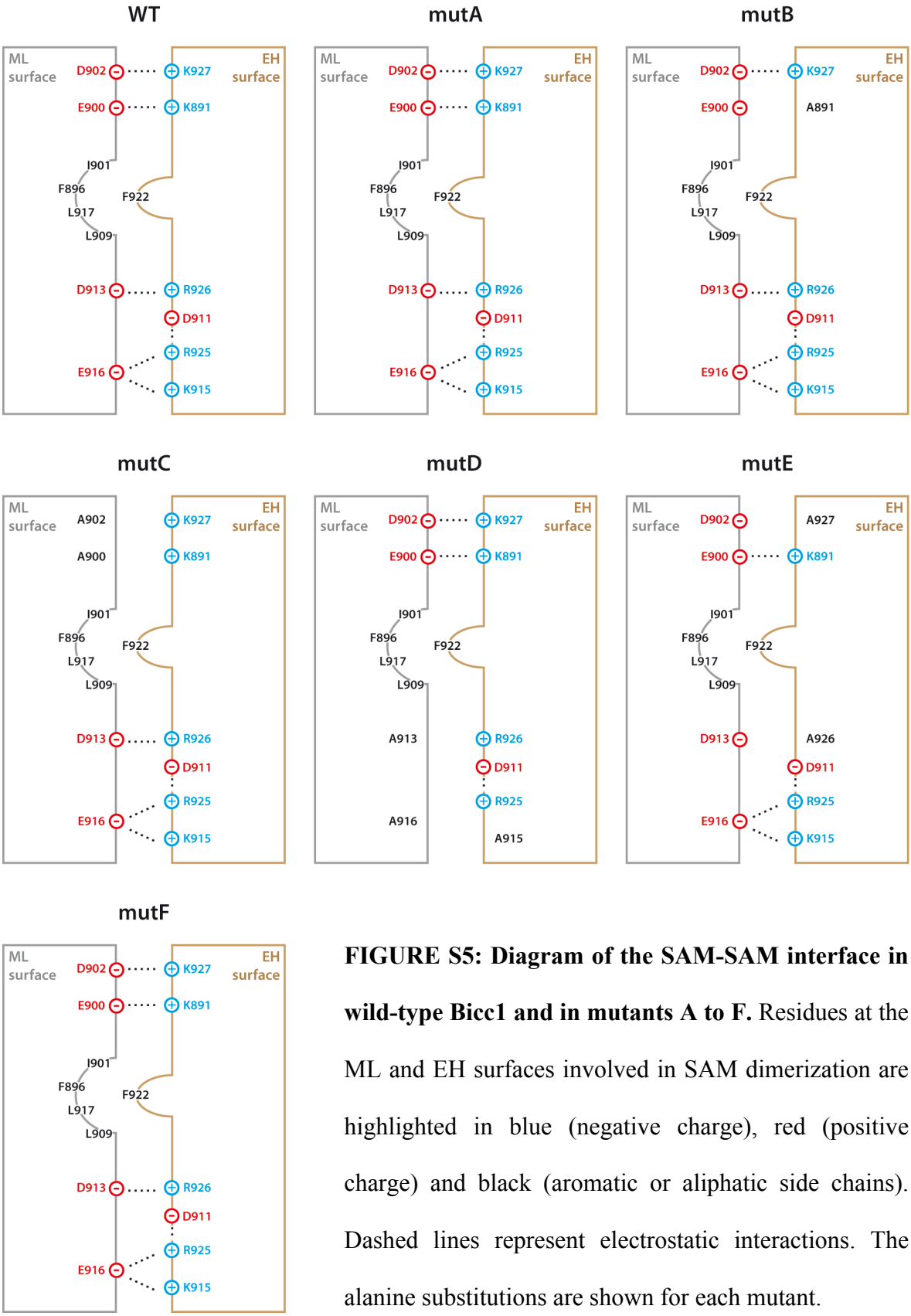

FIGURE S5: Diagram of the SAM-SAM interface in wild-type Bicc1 and in mutants A to F. Residues at the ML and EH surfaces involved in SAM dimerization are highlighted in blue (negative charge), red (positive charge) and black (aromatic or aliphatic side chains). Dashed lines represent electrostatic interactions. The alanine substitutions are shown for each mutant.

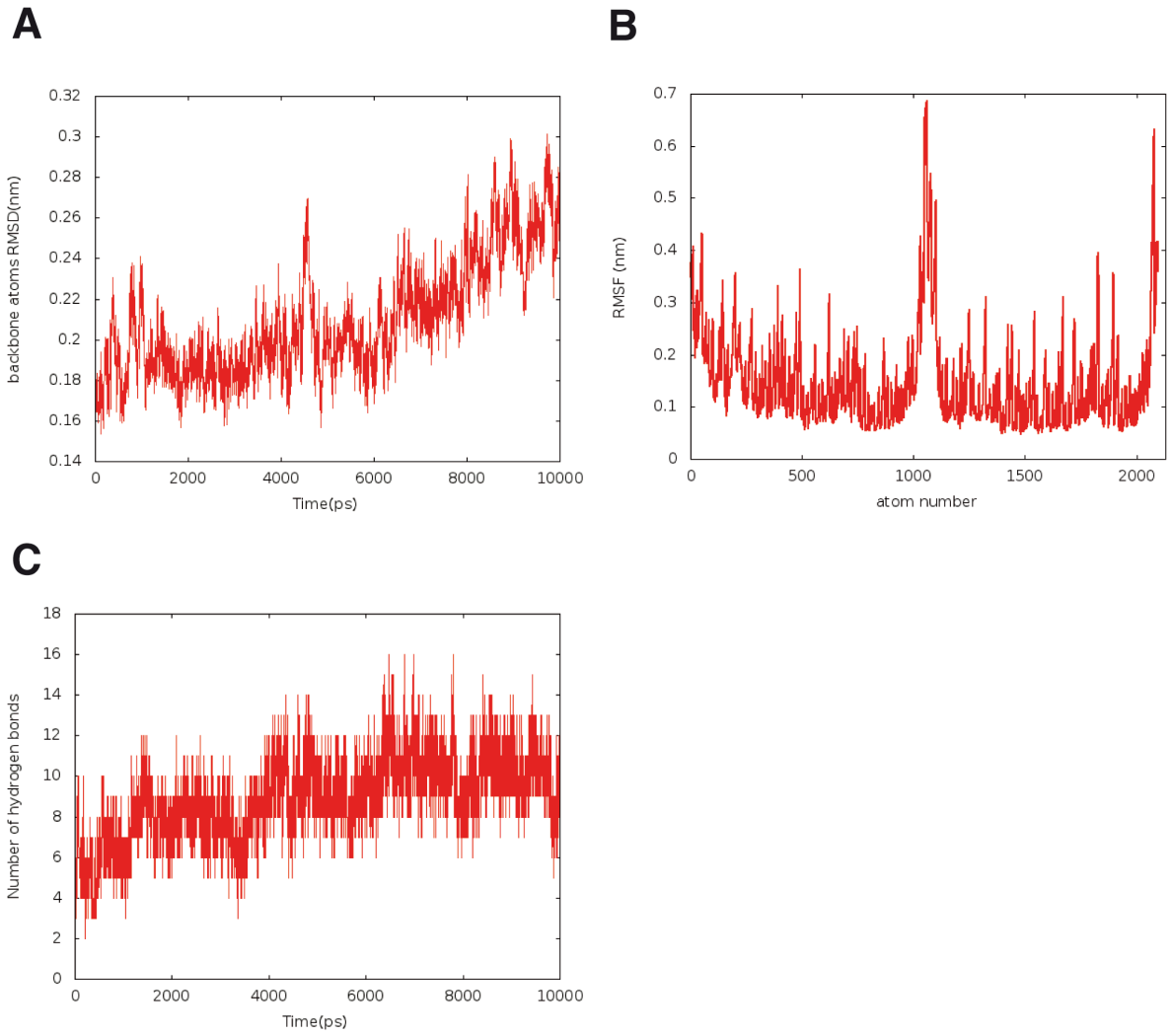

FIGURE S6: Molecular Dynamic parameters obtained for the Bicc1 SAM dimer model. (A) Plot of RMSD values per time frame obtained for the protein backbone. Frame 1 was used as reference. (B) Plot of RMS fluctuation per atom. The two SAM domains are considered as a single sequence, the central peak corresponds to the C-terminal extremity of the first domain followed by the N-terminal extremity of the second SAM domain. Initial frame was used as reference. (C) Plot of intermolecular H-bonds number counted per time frame.

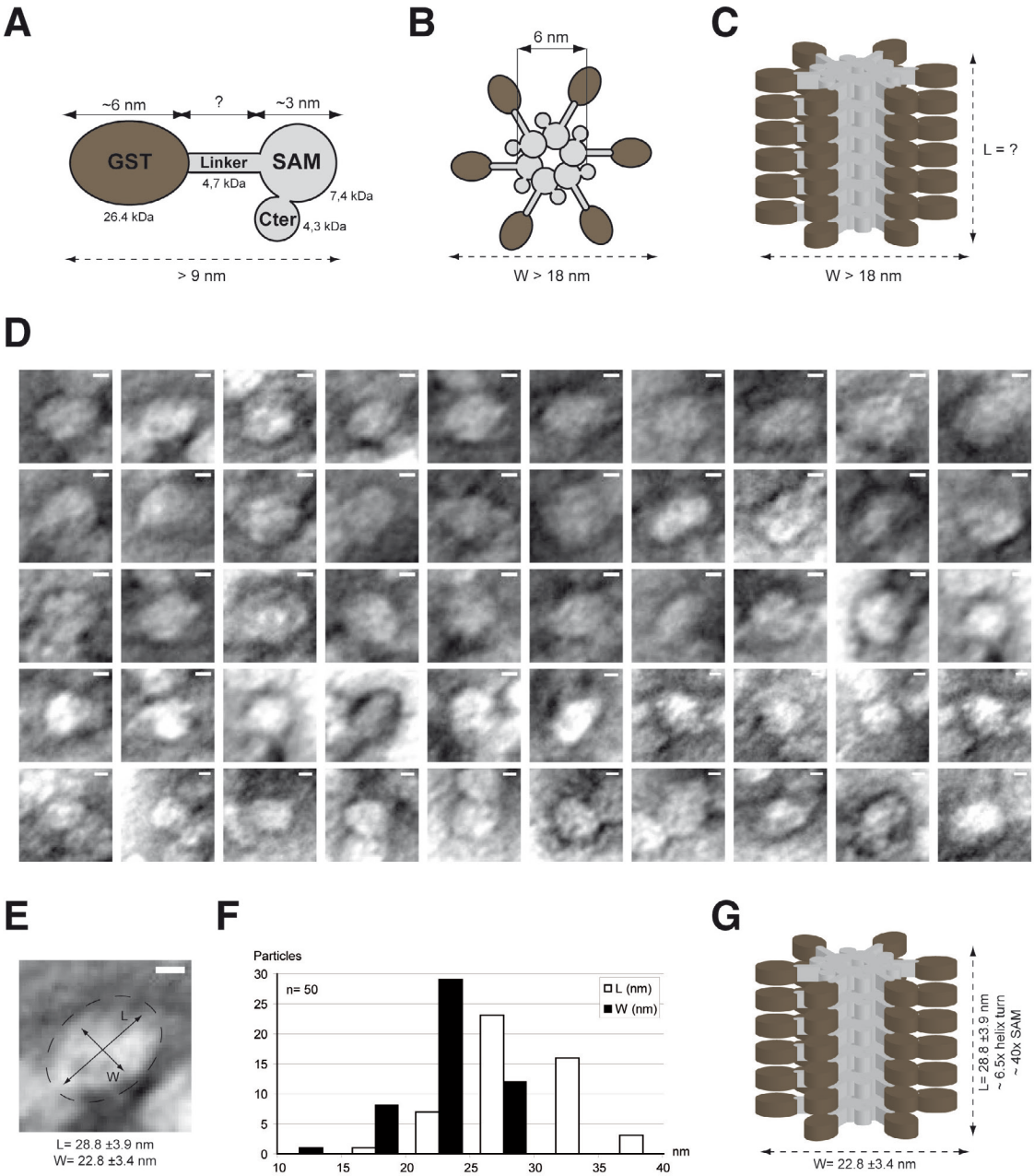

FIGURE S7: The GST-fused Bicc1 SAM domain form macromolecular self-assembly *in vitro.* (A) Schematic representation of the GST-SAM fusion protein. The approximate dimensions are given for each domain and for the whole protein. (B,C) Schematic representation of a GST-SAM polymer in section and longitudinal view, respectively. The expected dimensions are given. (D) Electron micrographs of recombinant GST-Bicc1-SAM revealed by negative staining. The 50 panels each represent one individual object observed by EM. (E) Graph showing the size distribution (length and width) of the ovoid structures detected by EM. (F) Schematic representation of a GST-SAM polymer in longitudinal view. The dimension displayed fit with the mean values measured for the ovoid structures detected by EM. (G) As in panel C, but with sizes extrapolated from panel D measurements.

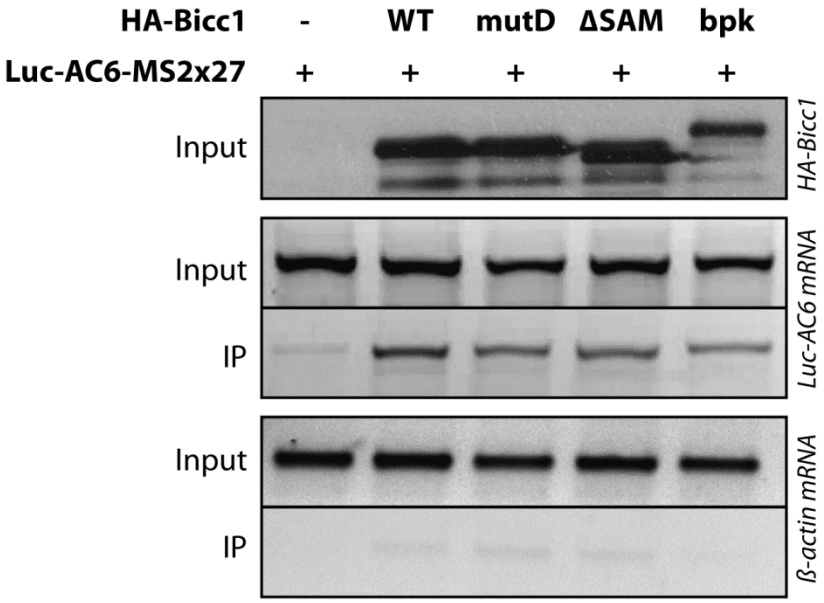

FIGURE S8: The Bicc1 polymer mutants mutD, ΔSAM and *bpk* remain competent to bind RNA. RNA co-immunoprecipitation. The Luc-AC6 reporter mRNA was expressed in HEK293T cells that were cotransfected with HA-Bicc1 or empty vector. After HA immunoprecipitation, the various fractions were analyzed by RT-PCR. 5% of the total extract was used as input. The ß-actin mRNA was used as negative control for the RT-PCR. A control Western blot shows the HA-Bicc1 level in 5% of the input used for RNA co-IP.